

# Solvent-Induced Chiroptical Changes in Supramolecular Assemblies of an Optically Active, Regioregular Polythiophene

Hidetoshi Goto,<sup>†</sup> Yoshio Okamoto,<sup>‡</sup> and Eiji Yashima<sup>\*†</sup>

Department of Molecular Design and Engineering and Department of Applied Chemistry,  
Graduate School of Engineering, Nagoya University, Chikusa-ku, Nagoya 464-8603, Japan

Received November 29, 2001; Revised Manuscript Received March 20, 2002

**ABSTRACT:** The solvent-induced chiroptical properties of an optically active, regioregular (head-to-tail) polythiophene bearing chiral oxazoline residues, poly[3-{4-((*R*)-4-ethyl-2-oxazolin-2-yl)phenyl}thiophene] (poly-**1a**), were investigated in mixtures of a good solvent, chloroform, and a variety of poor solvents by means of UV–visible and CD spectroscopies. Poly-**1a** exhibited an induced circular dichroism (ICD) in chloroform upon the addition of poor solvents such as methanol and acetone with similar Cotton effect patterns, while some poor solvents such as acetonitrile and nitromethane dramatically changed the Cotton effect patterns of poly-**1a**. The changes in the conformation, morphology, and the size of the poly-**1a** aggregates induced by different solvents were also investigated with <sup>1</sup>H NMR titrations, X-ray diffraction, filtration experiments using membrane filters, and atomic force microscopy (AFM) measurements. On the basis of these results, possible models for the chiral supramolecular aggregates are proposed.

## Introduction

$\pi$ -Conjugated polymers such as polythiophenes, polyphenylenes, and poly(phenylenevinylene)s self-assemble in solution or in the film and exhibit a color change due to the solvent (solvatochromism) and temperature (thermochromism).<sup>1,2</sup> Extensive investigations have been performed to apply such conjugated polymers to a macromolecular sensory system and as materials for electroluminescence (EL) devices.<sup>3</sup> On the other hand, chiral  $\pi$ -conjugated polymers bearing an optically active side group, particularly the chiral polythiophenes have recently attracted considerable interest due to their potential applications in enantioselective sensors, catalysts, and adsorbents.<sup>4</sup> In contrast to other optically active polymers, chiral polythiophenes usually exhibit no optical activity in the  $\pi$ – $\pi^*$  transition region in a good solvent but show unique optical activity in a poor solvent or in the film where they form a chiral, supramolecular self-assembly based on intermolecular  $\pi$ – $\pi$  stacking.<sup>4</sup> The chiral aggregates show an intense induced circular dichroism (ICD) in the UV–visible region derived from the main chain and/or supramolecular chirality.<sup>4</sup> However, it still remains difficult to elucidate the exact structure of the chiral aggregates.<sup>5</sup>

Recently, we reported that a novel, optically active regioregular polythiophene, poly[3-{4-((*R*)-4-ethyl-2-oxazolin-2-yl)phenyl}thiophene] (poly-**1a**), showed a unique ICD in the relatively shorter UV–visible wavelength region upon complexation with metal ions, such as copper(II) and iron(III), in a good solvent, chloroform for poly-**1a**.<sup>6</sup> The ICDs are completely different from previously reported ICDs based on chiral polythiophene aggregates due to intermolecular  $\pi$ -stacked interactions. We believe that the induced chirality for poly-**1a** may be derived from the main chain chirality, such as a predominantly one-handed helical conformation induced

by intermolecular coordination of the oxazoline group to metal ions. We also investigated the chiroptical properties of poly-**1a** in mixtures of chloroform and a variety of poor solvents using CD spectroscopy and found that the polymer exhibited dramatic changes in the sign and pattern of the ICDs of poly-**1a**.<sup>7</sup> This paper reports the detailed results of such unusual and interesting solvent effects on the ICDs by means of UV–visible and CD spectroscopies, NMR titrations, X-ray diffraction, filtration experiments, and AFM measurements.

## Experimental Section

**Materials.** Tetrahydrofuran (THF) (Kishida Chemical, Osaka, Japan, 99%) was dried over sodium benzophenone ketyl, distilled onto lithium aluminum hydride (LiAlH<sub>4</sub>) under nitrogen, and then distilled under high vacuum just before use. Toluene (Kishida, 99%), benzene (Wako Pure Chemical, Osaka, Japan, 99%), hexane (Wako, 95%), diethyl ether (Wako, 99%), and 1,4-dioxane (Wako, 99%) were distilled from sodium benzophenone ketyl under nitrogen. Chloroform (Kishida, 99%), dichloromethane (Kishida, 99%), acetone (Kishida, 99%), acetonitrile (Kishida, 99.5%), tetrachloromethane (Wako, 99.5%), ethyl acetate (Wako, 98%), and 1,5-cyclooctadiene (cod) (Wako, 98%) were dried over CaH<sub>2</sub> and distilled under nitrogen. Dimethyl sulfoxide (DMSO) (Kishida, 99%), *N,N*-Dimethylformamide (DMF) (Kishida, 99.5%), and *N*-methylformamide (Tokyo Kasei, Tokyo, Japan, 99%) were dried over CaH<sub>2</sub> and distilled under reduced pressure. Methanol (Nacalai Tesque, Kyoto, Japan, 99%), ethanol (Kyowa Sangyo, Nagoya, Japan, 99%), and 1-butanol (Wako, 98%) were dried over turning magnesium and iodine and distilled under nitrogen. Triethylamine (NET<sub>3</sub>) (Kishida, 99%), diethylamine (Wako, 99%), and diisopropylamine (Wako, 98%) were dried over KOH pellets, distilled under nitrogen, and stored under nitrogen over KOH pellets. Acetic acid (Kishida, 99.7%), nitromethane (Wako, 96%), and nitrobenzene (Kishida, 99.5%) were dried over CaCl<sub>2</sub> and distilled under nitrogen. Chloroform-*d* (99.8% D), acetone-*d*<sub>6</sub> (99.9% D), and acetonitrile-*d*<sub>3</sub> (99.8% D) obtained from Nippon Sanso (Tokyo, Japan) were dried over CaH<sub>2</sub>, distilled under nitrogen, and stored under nitrogen over molecular sieves 4A (Nacalai Tesque). Nitromethane-*d*<sub>3</sub> (Aldrich, 99% D) was used as received. Other solvents listed in Table 1 were dried over molecular sieves 4A.

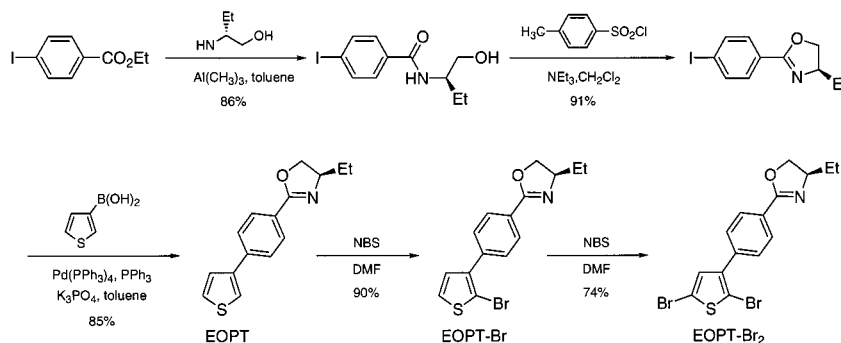
Trimethylaluminum (Me<sub>3</sub>Al) (1.0 M in *n*-hexane), *n*-butyllithium (*n*-BuLi) (1.54 M in *n*-hexane), bis(1,5-cyclooctadiene)-

\* To whom correspondence should be addressed. E-mail: yashima@apchem.nagoya-u.ac.jp.

<sup>†</sup> Department of Molecular Design and Engineering, Nagoya University.

<sup>‡</sup> Department of Applied Chemistry, Nagoya University.

Scheme 1. Synthesis of Monomers



nickel(0) ( $\text{Ni}(\text{cod})_2$ ) (95%), and 2,2'-bipyridyl (bpy) (99%) were purchased from Kanto Kagaku (Tokyo, Japan). Ethyl 4-iodobenzoate (97%), tetrakis(triphenylphosphine)palladium(0) ( $\text{Pd}(\text{PPh}_3)_4$ ), and [1,3-bis(diphenylphosphino)propane]dichloronickel(II) ( $\text{Ni}(\text{dppp})\text{Cl}_2$ ) (97%) were from Tokyo Kasei. 4-Toluenesulfonyl chloride (98%),  $\text{K}_3\text{PO}_4$  (97%), and *N*-bromosuccinimide (NBS) (98%) were obtained from Kishida. 3-Thiopheneboronic acid, magnesium bromide diethyl etherate ( $\text{MgBr}_2 \cdot \text{Et}_2\text{O}$ ) (99%), and (*S*)-2-butanol (99%) were from Aldrich. (*R*)-2-Amino-1-butanol (98%, 98%ee) and (*R*)-2-butanol (99%) were purchased from AZmax (Chiba, Japan) and Nacalai Tesque, respectively.

**Measurements.**  $^1\text{H}$  (500 MHz) and  $^{13}\text{C}$  (125 MHz) NMR spectra were measured on a Varian VXR-500S spectrometer using tetramethylsilane (TMS) as an internal standard. IR spectra were recorded using a Jasco Fourier transform IR-620 spectrophotometer. Absorption spectra were taken on a Jasco V-570 spectrophotometer. CD spectra were measured using a Jasco J-725 spectropolarimeter. Linear dichroism (LD) spectra were measured with a Jasco J-725 spectropolarimeter with an LD attachment. The concentration of poly-**1a** was calculated based on monomer units. Size exclusion chromatography (SEC) was performed with a Jasco PU-980 liquid chromatograph equipped with a Jasco DG-980-50 degasser and UV-visible detector (254 nm; Jasco UV-970) at 40 °C. An SEC column (Tosoh TSK-GEL Multipore H<sub>XL</sub>-M:  $30 \times 0.78$  cm (i.d.): pore size, 0.01–0.6  $\mu\text{m}$ ; bead size, 5  $\mu\text{m}$ ) was connected, and chloroform was used as eluent at a flow rate of 1.0 mL/min. The molecular weight calibration curve was obtained with standard polystyrenes (Tosoh). X-ray diffraction measurements were carried out with a RIGAKU RINT-1200, and the Cu  $K\alpha$  radiation was taken for the incident X-ray beam. AFM measurements were performed on a Nanoscope IIIa microscope (Digital Instruments) using standard silicon tips in the tapping mode. Height and phase images were simultaneously measured at the resonance frequency of the tips with 125  $\mu\text{m}$  long cantilevers (255–265 kHz).

**Monomer Synthesis.** The thiophene derivatives were synthesized according to Scheme 1.

**(*R*)-*N*-(4-Iodobenzoyl)-2-amino-1-butanol.**  $\text{Me}_3\text{Al}$  (385 mL, 385 mmol) in *n*-hexane (1.0 M) was added dropwise via a cannula to a toluene solution (550 mL) of (*R*)-2-amino-1-butanol (21 mL, 0.22 mol) at 0 °C under dry nitrogen. The reaction mixture was allowed to warm to room temperature and further stirred for 1.5 h. Ethyl 4-iodobenzoate (50 g, 0.18 mol) in toluene (150 mL) was added dropwise, and the mixture was heated under reflux for 41 h. After cooling to room temperature, a 20% aqueous solution of Rochelle salt (30 mL) was added to the reaction mixture. After filtration, the precipitate was dissolved in ethanol and the solvent was removed by evaporation. The resulting white needle crystals of (*R*)-*N*-(4-iodobenzoyl)-2-amino-1-butanol were then washed with water and dried over phosphorus pentoxide in vacuo at room temperature overnight (49.8 g, 86%). Mp: 146.5–147.2 °C.  $[\alpha]_{\text{D}}^{25}$ : +22.8° ( $c = 2.07$  g/dL in ethanol). IR (KBr,  $\text{cm}^{-1}$ ): 3375, 3301 ( $\nu_{\text{N-H}}$  or  $\text{O-H}$ ), 3081, 2968 ( $\nu_{\text{C-H}}$ ), 2873, 1639 ( $\nu_{\text{C=O}}$ ), 1587 ( $\nu_{\text{C=C}}$ ), 1543, 1331, 1049 ( $\nu_{\text{C-O}}$ ), 877, 715.  $^1\text{H}$  NMR ( $\text{CDCl}_3$ ):  $\delta$  1.00 (t,  $\text{CH}_3$ ,  $J = 7.4$  Hz, 3H), 1.56–1.76 (m,  $\text{CH}_3\text{CH}_2$ , 2H), 2.33 (s, OH, 1H), 3.70 (m,  $\text{OCH}_2$ , 1H), 3.78 (m,  $\text{OCH}_2$ , 1H), 4.05 (m, CH, 1H), 6.22 (s, NH, 1H), 7.48 (d,

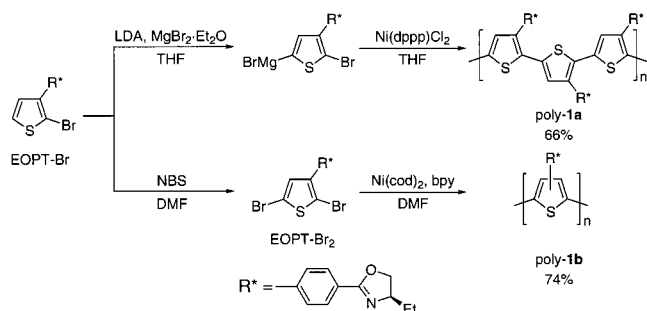
aromatic,  $J = 8.4$  Hz, 2H), 7.77 (d, aromatic,  $J = 8.4$  Hz, 2H). Anal. Calcd for  $\text{C}_{11}\text{H}_{14}\text{INO}_2$ : C, 41.40; H, 4.42; N, 4.39. Found: C, 41.32; H, 4.22; N, 4.32.

**(*R*)-4-Ethyl-2-(4-iodophenyl)-2-oxazoline.** A dichloromethane solution (100 mL) of 4-toluenesulfonyl chloride (38.3 g, 201 mmol) was added dropwise to a solution of (*R*)-*N*-(4-iodobenzoyl)-2-amino-1-butanol (49.4 g, 155 mmol) prepared above in dichloromethane (550 mL) and  $\text{NEt}_3$  (60 mL, 430 mmol) at 0 °C under nitrogen. The solution was then stirred at room temperature for 70 h. The dichloromethane solution was washed with saturated aqueous  $\text{NH}_4\text{Cl}$  and dried over  $\text{MgSO}_4$ . After the solvent was evaporated, the crude product was purified by silica gel chromatography with hexanes–ethyl acetate (10/1, v/v) as the eluent to give 42.3 g of (*R*)-4-ethyl-2-(4-iodophenyl)-2-oxazoline as white needles in 91% yield. Mp: 41–42 °C.  $[\alpha]_{\text{D}}^{25}$ : +54.7° ( $c = 1.01$  g/dL in chloroform). IR (KBr,  $\text{cm}^{-1}$ ): 2956 ( $\nu_{\text{C-H}}$ ), 2930 ( $\nu_{\text{C-H}}$ ), 2872, 1645 ( $\nu_{\text{C=N}}$ ), 1588 ( $\nu_{\text{C=C}}$ ), 1483, 1460, 1393, 1348, 1332, 1071 ( $\nu_{\text{C-O}}$ ), 1007, 897, 829, 728.  $^1\text{H}$  NMR ( $\text{CDCl}_3$ ):  $\delta$  0.99 (t,  $\text{CH}_3$ ,  $J = 7.4$  Hz, 3H), 1.62 (m,  $\text{CH}_3\text{CH}_2$ , 1H), 1.78 (m,  $\text{CH}_3\text{CH}_2$ , 1H), 4.06 (t,  $\text{OCH}_2$ ,  $J = 8.0$  Hz, 1H), 4.26 (m, CH, 1H), 4.48 (dd,  $\text{OCH}_2$ ,  $J = 9.6, 8.0$  Hz, 1H), 7.67 (d, aromatic,  $J = 6.8$  Hz, 2H), 7.76 (d, aromatic,  $J = 6.8$  Hz, 2H). Anal. Calcd for  $\text{C}_{11}\text{H}_{12}\text{INO}$ : C, 43.88; H, 4.02; N, 4.65. Found: C, 43.96; H, 4.07; N, 4.66.

**(*R*)-3-(4-(4-Ethyl-2-oxazolin-2-yl)phenyl)thiophene (EOPT).** (*R*)-4-Ethyl-2-(4-iodophenyl)-2-oxazoline (10.7 g, 35.4 mmol) was added to a mixture of 3-thiopheneboronic acid (5.02 g, 39.3 mmol),  $\text{Pd}(\text{PPh}_3)_4$  (1.23 g, 1.07 mmol), and  $\text{K}_3\text{PO}_4$  (25.0 g, 118 mmol) in toluene (140 mL) at room temperature. The reaction mixture was refluxed under nitrogen for 27 h. The solution was diluted with ether and the organic layer was washed with saturated aqueous  $\text{NH}_4\text{Cl}$ , and dried over  $\text{MgSO}_4$ . After the solvent was removed by evaporation, the residue was chromatographed on silica gel with hexanes–ethyl acetate (5/1, v/v) as the eluent to give 7.7 g of EOPT as white plate crystals in 85% yield. The enantiomeric excess of EOPT was estimated to be greater than 99% using an enantiomerically pure NMR shift reagent, europium tris[3-(trifluoromethylhydroxymethylene)-(+)-camphorate] ( $\text{Eu}(\text{tfc})_3$ ) in  $\text{CDCl}_3$  by  $^1\text{H}$  NMR spectroscopy. Mp: 104.5–105.0 °C.  $[\alpha]_{\text{D}}^{25}$ : +61.8° ( $c = 1.00$  g/dL in chloroform). IR (KBr,  $\text{cm}^{-1}$ ): 3017, 2957 ( $\nu_{\text{C-H}}$ ), 1641 ( $\nu_{\text{C=N}}$ ), 1359 ( $\nu_{\text{C-N}}$ ), 1260, 1071 ( $\nu_{\text{C-O}}$ ), 849, 786, 741.  $^1\text{H}$  NMR ( $\text{CDCl}_3$ ):  $\delta$  1.01 (t,  $\text{CH}_3$ ,  $J = 7.4$  Hz, 3H), 1.62 (m,  $\text{CH}_3\text{CH}_2$ , 1H), 1.78 (m,  $\text{CH}_3\text{CH}_2$ , 1H), 4.06 (t,  $\text{OCH}_2$ ,  $J = 8.0$  Hz, 1H), 4.26 (m, CH, 1H), 4.48 (dd,  $\text{OCH}_2$ ,  $J = 9.6, 8.0$  Hz, 1H), 7.40 (dd, thiophene- $\text{H}_5$ ,  $J = 5.0, 2.7$  Hz, 1H), 7.42 (dd, thiophene- $\text{H}_4$ ,  $J = 5.0, 1.5$  Hz, 1H), 7.53 (dd, thiophene- $\text{H}_2$ ,  $J = 2.7, 1.5$  Hz, 1H), 7.64 (d, aromatic,  $J = 8.4$  Hz, 2H), 7.76 (d, aromatic,  $J = 8.4$  Hz, 2H).  $^{13}\text{C}$  NMR ( $\text{CDCl}_3$ ):  $\delta$  10.00 ( $\text{CH}_3$ ), 28.61 ( $\text{CH}_3\text{CH}_2$ ), 67.97 ( $\text{OCH}_2$ ), 72.07 (CH), 121.27 (thiophene), 126.10 (aromatic), 126.41 (aromatic or thiophene), 126.47 (aromatic or thiophene), 128.72 (aromatic), 138.32 (aromatic), 141.38 (thiophene), 163.16 ( $\text{C=N}$ ). Anal. Calcd for  $\text{C}_{15}\text{H}_{15}\text{NOS}$ : C, 70.01; H, 5.87; N, 5.44. Found: C, 70.02; H, 5.93; N, 5.44.

**(*R*)-2-Bromo-3-(4-(4-ethyl-2-oxazolin-2-yl)phenyl)thiophene (EOPT-Br).** Regioselective bromination of EOPT was carried out according to a reported procedure<sup>8</sup> with a slight modification. NBS (4.52 g, 25.4 mmol) was added to a solution

## Scheme 2. Synthesis of Poly-1a and Poly-1b



of EOPT prepared above (6.23 g, 24.2 mmol) in DMF (39 mL) under nitrogen at room temperature under shielded light. After the mixture was stirred for 5 days, the solvent was evaporated, the residue was diluted with ether, and the solution was washed with water and then dried over  $\text{MgSO}_4$ . The solvent was removed by evaporation, and the residue was purified by silica gel chromatography with hexane–diethyl ether (10/1, v/v) as the eluent to give EOPT–Br (7.31 g, 90%) as a slightly yellow oil. IR (neat,  $\text{cm}^{-1}$ ): 3106, 2963 ( $\nu_{\text{C-H}}$ ), 2931 ( $\nu_{\text{C-H}}$ ), 1647 ( $\nu_{\text{C=N}}$ ), 1359 ( $\nu_{\text{C-N}}$ ), 1079, 1062 ( $\nu_{\text{C-O}}$ ), 1019, 988, 950, 872, 850, 719.  $^1\text{H NMR}$  ( $\text{CDCl}_3$ ):  $\delta$  1.01 (t,  $\text{CH}_3$ ,  $J = 7.4$  Hz, 3H), 1.63 (m,  $\text{CH}_3\text{CH}_2$ , 1H), 1.80 (m,  $\text{CH}_3\text{CH}_2$ , 1H), 4.09 (t,  $\text{OCH}_2$ ,  $J = 8.0$  Hz, 1H), 4.28 (m, CH, 1H), 4.51 (dd,  $\text{OCH}_2$ ,  $J = 9.4, 8.0$  Hz, 1H), 7.06 (d, thiophene- $\text{H}_5$ ,  $J = 5.6$  Hz, 1H), 7.42 (d, thiophene- $\text{H}_4$ ,  $J = 5.6$  Hz, 1H), 7.67 (d, aromatic,  $J = 8.4$  Hz, 2H), 7.76 (d, aromatic,  $J = 8.4$  Hz, 2H).  $^{13}\text{C NMR}$  ( $\text{CDCl}_3$ ):  $\delta$  10.01 ( $\text{CH}_3$ ), 28.63 ( $\text{CH}_3\text{CH}_2$ ), 68.02 ( $\text{OCH}_2$ ), 72.16 (CH), 109.28 (thiophene), 126.17 (thiophene), 127.00 (aromatic), 128.27 (aromatic), 128.50 (aromatic), 128.91 (thiophene), 137.73 (aromatic), 140.34 (thiophene), 163.12 ( $\text{C=N}$ ). Anal. Calcd for  $\text{C}_{15}\text{H}_{14}\text{BrNOS}$ : C, 53.58; H, 4.20; N, 4.17. Found: C, 53.58; H, 4.26; N, 4.20.

**(*R*)-2,5-Dibromo-3-(4-(4-ethyl-2-oxazolin-2-yl)phenyl)-thiophene (EOPT–Br<sub>2</sub>).** This compound was prepared by further bromination of EOPT–Br. NBS (0.665 g, 3.74 mmol) was added to a solution of EOPT–Br (0.968 g, 2.88 mmol) in DMF (4.6 mL) under nitrogen at room temperature. After the reaction mixture was stirred for 5 days under shielding light, the residue was diluted with ether, and the solution was washed with water and then dried over  $\text{MgSO}_4$ . The solvent was removed by evaporation, and the crude product was purified by silica gel chromatography with hexanes–ether (10/1, v/v) as the eluent to give EOPT–Br<sub>2</sub> (0.89 g, 74%) as white solids. Mp: 40–41 °C. IR (KBr,  $\text{cm}^{-1}$ ): 3054, 2962 ( $\nu_{\text{C-H}}$ ), 2934 ( $\nu_{\text{C-H}}$ ), 1645 ( $\nu_{\text{C=N}}$ ), 1356 ( $\nu_{\text{C-N}}$ ), 1063 ( $\nu_{\text{C-O}}$ ), 988, 855, 822.  $^1\text{H NMR}$  ( $\text{CDCl}_3$ ):  $\delta$  1.01 (t,  $\text{CH}_3$ ,  $J = 6.8$  Hz, 3H), 1.62 (m,  $\text{CH}_3\text{CH}_2$ , 1H), 1.78 (m,  $\text{CH}_3\text{CH}_2$ , 1H), 4.07 (t,  $\text{OCH}_2$ ,  $J = 8.0$  Hz, 1H), 4.26 (m, CH, 1H), 4.49 (dd,  $\text{OCH}_2$ ,  $J = 9.5, 8.0$  Hz, 1H), 7.04 (s, thiophene- $\text{H}_4$ , 1H), 7.54 (d, aromatic,  $J = 8.5$  Hz, 2H), 8.00 (d, aromatic,  $J = 8.5$  Hz, 2H).  $^{13}\text{C NMR}$  ( $\text{CDCl}_3$ ):  $\delta$  9.97 ( $\text{CH}_3$ ), 28.59 ( $\text{CH}_3\text{CH}_2$ ), 68.02 ( $\text{OCH}_2$ ), 72.19 (CH), 108.33 (thiophene), 111.54 (thiophene), 127.42 (aromatic), 128.33 (aromatic), 128.36 (aromatic), 131.43 (thiophene), 136.65 (aromatic), 141.18 (thiophene), 162.98 ( $\text{C=N}$ ). Anal. Calcd for  $\text{C}_{15}\text{H}_{13}\text{Br}_2\text{NOS}$ : C, 43.40; H, 3.16; N, 3.37. Found: C, 43.36; H, 3.15; N, 3.31.

**Polymerization.** Polymerization was carried out in a dry glass ampule under a dry nitrogen atmosphere according to Scheme 2.

**Polymerization of EOPT–Br with Ni(dppp)Cl<sub>2</sub> as a Catalyst (Poly-1a).** Polymerization of EOPT–Br was carried out according to McCullough's procedure<sup>9</sup> with a modification. EOPT–Br (2.29 g, 6.82 mmol) and  $\text{MgBr}_2\cdot\text{Et}_2\text{O}$  (2.03 g, 7.87 mmol) weighed under nitrogen were placed in a two-necked flask equipped with a magnetic stirrer bar and a three-way stopcock under dry nitrogen, and THF (44 mL) was added with a syringe. The mixture was cooled to  $-98$  °C, and an LDA solution (7.85 mmol based on *n*-BuLi used for the preparation of LDA) in THF (6.5 mL) was added to this suspension solution via a cannula under dry nitrogen at  $-98$  °C. After the mixture

was stirred for 10 min at  $-98$  °C, Ni(dppp)Cl<sub>2</sub> (18.5 mg, 34.1  $\mu\text{mol}$ ) was added, and the mixture was allowed to warm to room temperature slowly, whereupon (at ca.  $-40$  °C) the solution became clear. After 20 min, Ni(dppp)Cl<sub>2</sub> (18.5 mg, 34.1  $\mu\text{mol}$ ) was added to the reaction mixture, and the mixture was further stirred at room temperature for 20 min and Ni(dppp)Cl<sub>2</sub> (18.5 mg, 34.1  $\mu\text{mol}$ ) was added again. The mixture was then refluxed under stirring. After 62 h, the solvent was almost removed under reduced pressure, and the resulting purple-colored polymer was precipitated into a large amount of methanol, collected by centrifugation, washed with methanol and THF, and dried in vacuo at room temperature overnight. The polymer was then dissolved in chloroform and precipitated into a large amount of hexane, collected by centrifugation, and dried in vacuo at room temperature overnight (1.16 g, 66%). IR (KBr,  $\text{cm}^{-1}$ ): 3060, 2960 ( $\nu_{\text{C-H}}$ ), 2930 ( $\nu_{\text{C-H}}$ ), 1645 ( $\nu_{\text{C=N}}$ ), 1610 ( $\nu_{\text{C=C}}$ ), 1359 ( $\nu_{\text{C-N}}$ ), 1064 ( $\nu_{\text{C-O}}$ ), 835.  $^1\text{H NMR}$  ( $\text{CDCl}_3$ ):  $\delta$  1.0 (t,  $\text{CH}_3$ , 3H), 1.6–1.8 (m,  $\text{CH}_3\text{CH}_2$ , 2H), 4.0 (m,  $\text{OCH}_2$ , 1H), 4.2 (m, CH, 1H), 4.4 (m,  $\text{OCH}_2$ , 1H), 6.8–7.2 (m, thiophene- $\text{H}_4$ , 1H), 7.3–8.0 (m, aromatic, 4H). Anal. Calcd for  $(\text{C}_{15}\text{H}_{13}\text{NOS})_n$ : C, 70.56; H, 5.13; N, 5.49. Found: C, 70.56; H, 5.21; N, 5.31.  $M_n = 5.3 \times 10^3$ ,  $M_w/M_n = 1.3$ .

**Polymerization of EOPT–Br<sub>2</sub> with Ni(cod)<sub>2</sub> as a Catalyst (Poly-1b).** A mixture of Ni(cod)<sub>2</sub> (0.76 g, 2.8 mmol), cod (1.5 mL, 12 mmol), and bpy (0.40 g, 3.3 mmol) in DMF (20 mL) was added to a solution of EOPT–Br<sub>2</sub> (0.83 g, 2.0 mmol) in DMF (13 mL) under nitrogen, and the mixture was stirred at 100 °C for 62 h. After the solvent was almost removed under reduced pressure, the resulting orange-colored polymer was precipitated into a large amount of methanol, collected by centrifugation, washed with methanol, and dried in vacuo at room temperature overnight (0.38 g, 74%). IR (KBr,  $\text{cm}^{-1}$ ): 3061, 2961 ( $\nu_{\text{C-H}}$ ), 2927 ( $\nu_{\text{C-H}}$ ), 1647 ( $\nu_{\text{C=N}}$ ), 1610 ( $\nu_{\text{C=C}}$ ), 1359 ( $\nu_{\text{C-N}}$ ), 1065 ( $\nu_{\text{C-O}}$ ), 835.  $^1\text{H NMR}$  ( $\text{CDCl}_3$ ):  $\delta$  1.0 (s,  $\text{CH}_3$ , 3H), 1.6–1.8 (m,  $\text{CH}_2$ , 2H), 4.0 (m,  $\text{OCH}_2$ , 1H), 4.2 (m, CH, 1H), 4.4 (m,  $\text{OCH}_2$ , 1H), 6.8–8.0 (m, thiophene- $\text{H}_4$  and aromatic, 5H). Anal. Calcd for  $(\text{C}_{15}\text{H}_{13}\text{NOS}\cdot\text{Br}_{0.182})_n$ : C, 66.80; H, 4.96; N, 5.16. Found: C, 66.65; H, 5.24; N, 4.98.  $M_n = 3.4 \times 10^3$ ,  $M_w/M_n = 2.1$ .

**UV–Visible and CD Titrations of Poly-1a with Various Solvents Mixtures.** A typical experimental procedure is described below. A stock solution of poly-1a (4 mg/2 mL) in chloroform was prepared and the initial UV–visible and CD spectra were measured. A 50- $\mu\text{L}$  aliquot of the poly-1a solution was transferred to a 0.1 cm quartz cell with a stopcock using a Hamilton microsyringe. An appropriate volume of methanol and chloroform as the diluent (percent volumes of methanol were 50, 53, 55, 57, 60, and 65) was added so as to keep the total volume (400  $\mu\text{L}$ ) and the poly-1a concentration (0.25 mg/mL), and then the UV–visible and CD spectra were recorded. In a similar manner, the UV–visible and CD titrations of poly-1a with other various solvents were performed. For (*R*)- or (*S*)-2-butanol, 40  $\mu\text{L}$  of the poly-1a solution and 40  $\mu\text{L}$  of chloroform were placed in a 0.1 cm quartz cell. To this was added increasing volumes of (*R*)- or (*S*)-2-butanol (80–320  $\mu\text{L}$ ), and the UV–visible and the CD spectra were measured for each addition of 2-butanol.

**$^1\text{H NMR}$  Titrations of Poly-1a with Various Solvents.** A typical experimental procedure is described below. A stock solution of poly-1a (4 mg/2 mL) in  $\text{CDCl}_3$  was prepared, 500  $\mu\text{L}$  of the poly-1a solution was transferred to a 5 mm NMR tube with a Hamilton microsyringe, and the initial  $^1\text{H NMR}$  spectrum was recorded at ambient temperature (ca. 22–24 °C). Increasing volumes of acetone- $d_6$  (0–220  $\mu\text{L}$ ) were added, and the  $^1\text{H NMR}$  spectra were taken for each addition of acetone- $d_6$ . The same procedure was followed for acetonitrile- $d_3$  and nitromethane- $d_3$ , respectively.

**X-ray Diffraction of Poly-1a.** A stock solution of poly-1a (150 mg/30 mL) in chloroform was prepared and filtered with a 0.50  $\mu\text{m}$  membrane filter. After 10 mL of the stock solution was transferred to three 30 mL flasks equipped with a stopcock, 10 mL of acetonitrile, methanol, or acetone was added to each flask, and the solutions were cooled slowly in a refrigerator to obtain the polymer powders. The chloroform



solution of poly-**1a** was also cast on glass substrates to prepare a polymer film.

**Filtration Experiments of Poly-1a with Various Solvents.** Advantec membrane filters (pore size: 0.50, 0.20, and 0.10  $\mu\text{m}$ ) (Toyo Roshi Co. Ltd., Japan) and Whatman biofilter (pore size: 0.02  $\mu\text{m}$ ) were used. In a typical experimental procedure, a stock solution of poly-**1a** (10 mg/100 mL) in chloroform was prepared and the initial UV-visible and CD spectra were measured. The poly-**1a** solution (5 mL) was transferred to a 10 mL flask equipped with a stopcock using a pipet. An appropriate volume of acetone was added and the resulting solution was diluted with chloroform (percent volumes of acetone were 25, 30, 35, and 50) so as to keep the total volume (10 mL) and the poly-**1a** concentration (0.05 mg/mL), and then the UV-visible and CD spectra were recorded. After each solution was filtered with the membrane filters, the absorption and CD spectra of the filtrates were recorded. In a similar manner, filtration experiments of poly-**1a** with acetonitrile and nitromethane were performed.

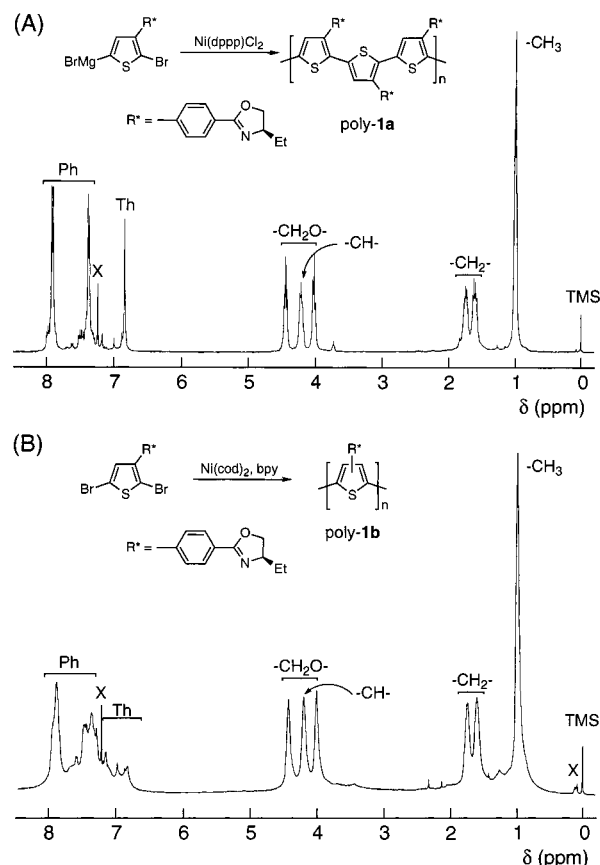
**AFM Measurements of Poly-1a Aggregates.** A stock solution of poly-**1a** (10 mg/100 mL) in chloroform was prepared and filtered with a 0.50  $\mu\text{m}$  membrane filter. A 1 mL aliquot of the stock solution of poly-**1a** was transferred to three 2 mL flasks equipped with a stopcock. One milliliter each of acetone, acetonitrile, and nitromethane was added to these flasks, respectively, and the solutions were cast on freshly cleaved mica substrates. The solvent was evaporated simultaneously in a stream of nitrogen. The same procedure was performed in the AFM measurements of poly-**1a** aggregates in a chloroform-methanol mixture with a poly-**1a** (0.5 mL, 0.2 mg/mL) solution in chloroform and 1.5 mL of methanol.

**Molecular Modeling and Calculations.** Molecular modeling and molecular mechanics calculation were performed with the Dreiding force field (version 2.21)<sup>10</sup> as implemented in CERIUS<sup>2</sup> software (version 3.8; Molecular Simulations Inc., Burlington, MA) running on an Indigo-Extreme graphics workstation (Silicon Graphics). The polymer model (20 repeating units of monomer units) of poly-**1a** was constructed using a Polymer Builder module in CERIUS<sup>2</sup>. Charges on atoms of poly-**1a** were calculated using charge equilibration (QEq) in CERIUS<sup>2</sup>; total charge of the molecule was zero. The starting main chain conformation of a polymer model was defined as a conformation of a rotational single bond between neighboring thiophene rings. The initial dihedral angle of a single bond from planarity was set to 180° (all anti). The constructed models were accomplished by conjugate gradient method. The energy minimization was continued until the root-mean-square (rms) value became less than 0.1 kcal mol<sup>-1</sup> Å<sup>-1</sup>.

## Results and Discussion

**Synthesis of Monomers and Polymers.** The chiral thiophene derivatives bearing an optically active oxazoline residue and the polythiophenes (poly-**1a** and poly-**1b**) with different regioregularities were synthesized as outlined in Schemes 1 and 2. First, ethyl 4-iodobenzoate was reacted with (*R*)-2-amino-1-butanol in the presence of Me<sub>3</sub>Al in toluene to yield an optically active hydroxy amide derivative.<sup>11</sup> The hydroxy amide derivative was then converted to the corresponding chiral oxazoline derivative by treatment with 4-toluenesulfonyl chloride in dichloromethane containing NEt<sub>3</sub>.<sup>11</sup> The oxazoline derivative was cross-coupled to 3-thiopheneboronic acid by Suzuki coupling<sup>12</sup> with Pd(PPh<sub>3</sub>)<sub>4</sub> in the presence of K<sub>3</sub>PO<sub>4</sub> in toluene to give EOPT in 85% yield. EOPT-Br was prepared through the selective bromination of EOPT at the 2-position of the thiophene ring with NBS in DMF.<sup>8</sup> EOPT-Br<sub>2</sub> was also obtained by the bromination of EOPT-Br at the 5-position of the thiophene ring under similar conditions.

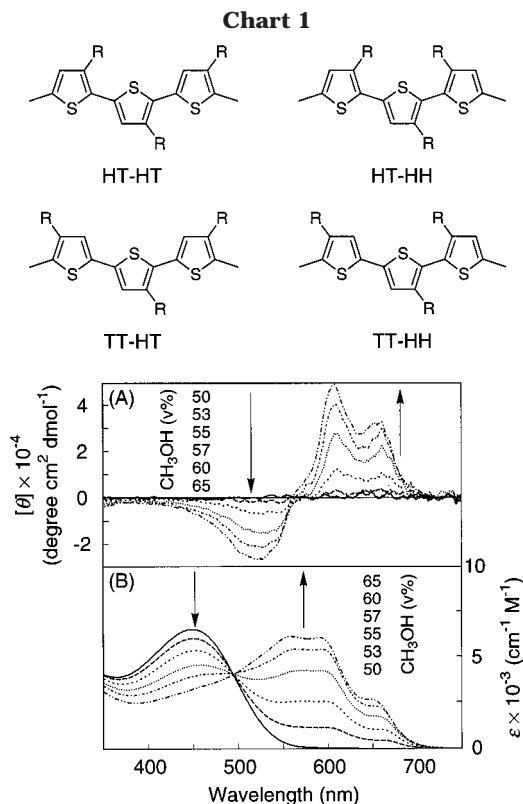
The regioregular polythiophene, poly-**1a**, was synthesized from EOPT-Br using McCullough's method (Scheme 2).<sup>6,9</sup> The regiorandom polythiophene, poly-**1b**,



**Figure 1.** <sup>1</sup>H NMR (500 MHz) spectra of poly-**1a** (A) and poly-**1b** (B) in CDCl<sub>3</sub> at ambient temperature (ca. 22–24 °C). X denotes protons derived from solvents and impurities.

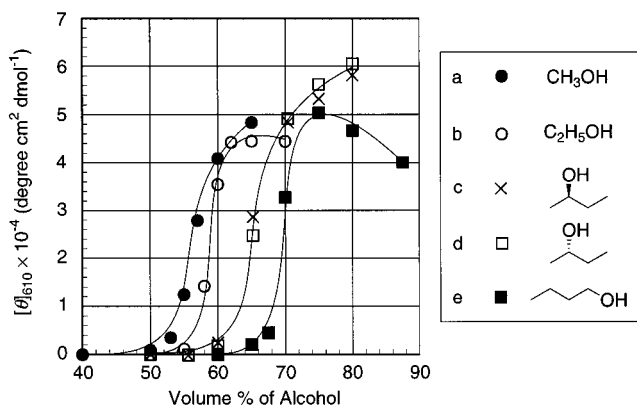
was also prepared from EOPT-Br<sub>2</sub> for comparison using a nickel-catalyzed homocoupling method.<sup>6,13</sup> Both polymers are soluble in chloroform and were isolated and purified as methanol-insoluble fractions. Poly-**1a** is insoluble in other common organic solvents, including acetone, acetonitrile, nitromethane, THF, and DMSO. The molecular weights (*M<sub>n</sub>*) and distributions (*M<sub>w</sub>*/*M<sub>n</sub>*) of poly-**1a** and poly-**1b** were determined to be  $5.3 \times 10^3$  and  $3.4 \times 10^3$  and 1.3 and 2.1, respectively, by SEC (polystyrene standards) using chloroform as the eluent. The relatively low molecular weights of these polymers may be due to precipitation in the solvents during the polymerization, thus preventing further propagation reactions. The <sup>1</sup>H NMR spectra of these polymers in CDCl<sub>3</sub> were measured to gain information regarding the regioregularities (Figure 1). The <sup>1</sup>H NMR spectrum of poly-**1a** in CDCl<sub>3</sub> showed a sharp singlet spectrum centered at 6.84 ppm derived from the 4-position proton on the thiophene ring, indicating that poly-**1a** possesses a regioregular head-to-tail (HT) structure (Chart 1); the HT-HT content was estimated to be more than 90% based on the <sup>1</sup>H NMR spectroscopy.<sup>14</sup> The small resonances of poly-**1a** in the aromatic region may be identified as those of oligomers and the end groups of the polymer.<sup>15</sup> On the other hand, poly-**1b** showed very broad <sup>1</sup>H NMR signals due to the lower regioregularity of the main chain structure.

**CD and Absorption Spectra of Poly-1a in Various Solvents Mixtures.** The chiroptical properties of the optically active, regioregular polythiophene, poly-**1a**, were examined using CD and absorption spectroscopies. Similar to the chiral regioregular polythiophenes reported so far,<sup>4</sup> poly-**1a** also showed no ICD



**Figure 2.** CD (A) and absorption (B) spectral changes of poly-**1a** in chloroform–methanol mixtures. The CD spectra were measured in a 0.1 cm quartz cell at ambient temperature (ca. 22–24 °C) with a poly-**1a** concentration of 0.25 mg (1.0  $\mu$ mol monomer units)/mL.

in the UV–visible region of the main chain over a temperature range (–40 to +25 °C) in a good solvent, chloroform. On the other hand, upon the addition of a poor solvent such as methanol (50–65%, v/v) to the chloroform solution of poly-**1a**, the polymer associated with form a chiral aggregate and exhibited an intense, split-type ICD with a positive first Cotton effect and a negative second Cotton effect in the absorption region. The color of the solution spontaneously changed from yellow-orange to violet. The CD and absorption spectral changes of poly-**1a** in the mixtures of chloroform and methanol are shown in Figure 2. In accordance with appearance of the ICDs, the absorption spectra of poly-**1a** showed a large red shift up to ca. 200 nm and exhibited a series of vibronic transitions at  $\lambda_{\text{max}} = 558$ , 590, and 650 nm with a clear-cut isosbestic point at 494 nm. Similar solvatochromisms and concomitant CD inductions were also observed for other chiral regio-regular polythiophenes and are considered to be due to a transformation from a disordered, coil-like form to an ordered, rod-like  $\pi$ -stacked one in order to form a chiral supramolecular self-assembly with interchain  $\pi$ – $\pi^*$  interactions of the polythiophene main chain.<sup>4</sup> We also measured the LD spectra of poly-**1a** in the mixtures of chloroform and methanol and found that the LD contributions are negligible. On the other hand, the regio-random poly-**1b** showed very weak ICDs in the presence of excess methanol (over 90%) at a longer wavelength accompanied by slight changes in the absorption spectra. These results indicate that the control of the regioregularity of the main chain is one of the most important factors to induce a chiral supramolecular aggregate as already reported for other chiral polythiophenes.<sup>4</sup>



**Figure 3.** Changes in CD intensity of poly-**1a** at 610 nm in chloroform–alcohol mixtures at ambient temperature (ca. 22–24 °C) with a poly-**1a** concentration of 0.25 mg (1.0  $\mu$ mol monomer units)/mL (a, b, e) and 0.20–0.89 mg (0.8–3.5  $\mu$ mol monomer units)/mL (c, d).

Next, we investigated the influence of the structures of alcohols on the ICD appearance for poly-**1a**. Upon the addition of a variety of achiral and chiral alcohols such as ethanol, 1-butanol, and (*R*)- and (*S*)-2-butanol, poly-**1a** also showed an intense ICD in the  $\pi$ – $\pi^*$  transition region and the ICD patterns were almost the same as those in the chloroform–methanol mixtures. However, the necessary volumes of alcohols to induce an ICD on the polymer were different, and they increased as the hydrophobicity of the alcohols increased (Figure 3). The enantiomeric (*R*)- and (*S*)-2-butanol induced similar ICDs on poly-**1a**.

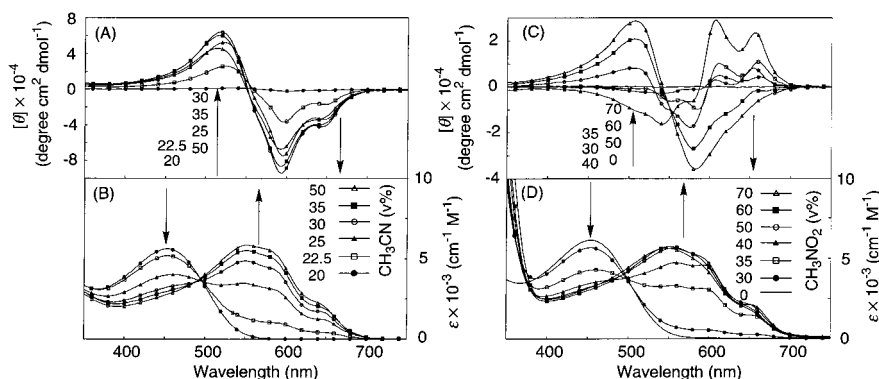
We also examined the solvent effects (steric and polarity effects) on the ICDs of poly-**1a** using a variety of solvents (protic, aprotic dipolar, and aprotic apolar solvents)<sup>16,17</sup> such as alcohols, hydrocarbons, ethers, amines, ketones, acids, esters, amides, sulfoxides, nitriles, and nitro compounds (Tables 1 and 2). Upon the addition of poor solvents to the poly-**1a** solution in chloroform, poly-**1a** also showed similar ICDs regardless of the properties of the poor solvents, and the ICD patterns were almost the same as those in the chloroform–methanol mixtures. Benzene and dichloromethane, in which poly-**1a** was not dissolved, induced no ICDs on poly-**1a** in the UV–visible region.

Some poor solvents such as acetonitrile and nitromethane brought about dramatic changes in the ICD patterns of poly-**1a** (Figure 4).<sup>7</sup> Although the changes in the absorption spectra of poly-**1a** in the chloroform–acetonitrile mixtures (20–50%, v/v) were almost the same as those in the chloroform–methanol mixtures and the color changed from yellow-orange to purple, the Cotton effect signs on the ICDs were completely reversed. The ICD intensity slightly decreased with an increase in the acetonitrile content (30–50% in Figure 4A), probably because poly-**1a** chains may stack efficiently to form a face-to-face  $\pi$ -stacked complex in the acetonitrile–chloroform mixture. Meijer et al. and Fujiki et al. reported similar dramatic solvent effects by chiral polythiophenes,<sup>18</sup> poly(phenylenevinylene)s,<sup>19</sup> and poly(alkylarylsilane)s<sup>20</sup> on the ICDs. We then examined the CD and absorption spectral changes of poly-**1a** using a variety of nitrile derivatives such as propionitrile, butyronitrile, acrylonitrile, crotonitrile, and benzonitrile. However, the ICD patterns were similar to those in the chloroform–methanol mixtures and opposite to those in the chloroform–acetonitrile mixtures. Upon the addition of acetonitrile-*d*<sub>3</sub>, poly-**1a** exhibited the same

**Table 1.** CD and Absorption Spectral Data of Poly-1a in Chloroform–Various Solvent Mixtures at ca. 22–24 °C<sup>a</sup>

| solvent  | $\epsilon_r$ (25 °C) <sup>b</sup> | $v\%$ <sup>c</sup> | CD spectra<br>([ $\theta$ ] $\times 10^{-4}$ (deg cm <sup>2</sup> dmol <sup>-1</sup> )/ $\lambda$ (nm) <sup>d</sup> |           |               | absorption spectra      |        |                       |          |
|--|-----------------------------------|--------------------|---|-----------|---------------|-------------------------|--------|-----------------------|----------|
|  |                                   |                    | first cotton  |           | second cotton | $\lambda_{\max}^d$ (nm) |        | isosbestic point (nm) |          |
| methanol   | 32.66                             | 65                 | 3.31/661  | 4.94/608  | -2.69/523     | 650                     | 590    | 558                   | 494      |
| ethanol  | 24.55                             | 70                 | 3.07/661  | 4.64/606  | -2.61/526     | 650                     | 592    | 558                   | 497      |
| 1-butanol  | 17.51                             | 75                 | 2.75/652  | 5.15/608  | -2.44/526     | 650                     | 593    | 558                   | 493      |
| ( <i>R</i> )-2-butanol <sup>e</sup>              | 16.56                             | 80                 | 4.67/659  | 6.07/608  | -3.25/532     | 651                     | 595    | 557                   | 495      |
| ( <i>S</i> )-2-butanol <sup>e</sup>              | 16.56                             | 80                 | 4.48/659  | 5.91/608  | -3.29/531     | 651                     | 595    | 555                   | 495      |
| 2,2,2-trifluoroethanol <sup>f</sup>              |                                   |                    |   |           |               |                         |        |                       |          |
| acetic acid <sup>f</sup>                         | 6.17 (20 °C)                      |                    |   |           |               |                         |        |                       |          |
| acetonitrile <sup>g</sup>                        | 35.94                             | 30                 | -4.22/643   | -9.40/594 | 6.41/518      | 650 sh                  | 590 sh | 552                   | 497      |
| acetonitrile- <i>d</i> <sub>3</sub> <sup>g</sup> |                                   | 30                 | -4.04/644   | -9.18/593 | 6.35/517      | 650 sh                  | 590 sh | 552                   | 496      |
| fluoroacetonitrile <sup>g</sup>                  |                                   | 30                 | -0.20/651   | -0.31/601 | 0.18/540      | 650 sh                  | 597    | 562                   | 498      |
| chloroacetonitrile <sup>h</sup>                  |                                   | 25                 | 0.15/550  | -3.13/475 | 3.99/417      | 415                     |        |                       | 430      |
|  |                                   | 50                 | 0.54/527  | -1.09/448 |               | 545                     |        |                       | 430, 360 |
|  |                                   | 87.5               | 0.35/535  | -0.93/466 | 0.50/408      | 450                     |        |                       |          |
| bromoacetonitrile                                |                                   | 60                 | 2.16/657  | 2.80/608  | -1.57/437     | 650 sh                  | 597    | 561                   | 498      |
| iodoacetonitrile <sup>i</sup>                    |                                   |                    |   |           |               | 572 sh                  |        |                       |          |
| propionitrile                                    | 28.86 (20 °C)                     | 30                 | 2.82/656  | 3.94/607  | -2.30/531     | 652                     | 596    | 559                   | 495      |
| butyronitrile                                    | 20.30 (21 °C)                     | 50                 | 2.70/651  | 4.06/603  | -2.28/522     | 650                     | 589    | 558                   | 495      |
| acrylonitrile                                    |                                   | 40                 | 2.84/655  | 4.02/606  | -2.33/530     | 652                     | 595    | 560                   | 497      |
| crotononitrile                                   |                                   | 50                 | 2.95/653  | 4.20/605  | -2.40/527     | 652                     | 597    | 559                   | 496      |
| benzonitrile                                     | 25.20                             | 87.5               | 2.75/656  | 4.10/606  | -2.44/523     | 651                     | 594    | 558                   | 498      |
| nitromethane <sup>j</sup>                        | 35.94                             | 40                 | 2.34/656  | 2.89/608  | -1.62/542     | 650                     | 592    | 558                   | 498      |
|  |                                   | 70                 | -3.59/582   |           | 2.87/507      | 650 sh                  | 590 sh |                       |          |
| nitrobenzene                                     | 34.78                             | 87.5               | 0.95/658  | 1.30/610  | -0.84/529     | 650 sh                  | 590 sh | 560 sh                | 497      |
| <i>N</i> -methylformamide                        | 182.4                             | 60                 | 2.23/653  | 3.48/603  | -1.90/524     | 653                     | 595    | 563                   | 498      |
| <i>N,N</i> -dimethylformamide                    | 36.71                             | 30                 | 3.00/656  | 4.16/606  | -2.37/530     | 652                     | 596    | 558                   | 499      |
| dimethyl sulfoxide                               | 46.45                             | 30                 | 2.62/653  | 3.81/605  | -2.29/524     | 649                     | 593    | 560                   | 499      |
| acetone  | 20.56                             | 35                 | 3.32/658  | 4.76/600  | -2.57/529     | 651                     | 593    | 557                   | 497      |
| ethyl acetate                                    | 6.02                              | 50                 | 2.79/649  | 4.42/602  | -2.58/518     | 645                     | 590    | 556                   | 495      |
| 1,4-dioxane                                      | 2.21                              | 50                 | 0.18/652  | 0.26/605  | -0.18/533     | 650 sh                  | 590 sh | 560 sh                | <i>k</i> |
| tetrahydrofuran                                  | 7.58                              | 50                 | 1.33/657  | 1.69/609  | -1.16/540     | 654                     | 597    | 560 sh                | <i>k</i> |
| diethyl ether                                    | 4.20                              | 50                 | 2.90/650  | 4.43/602  | -2.51/518     | 645                     | 591    | 556                   | 498      |
| diethylamine                                     | 3.78                              | 50                 | 3.05/650  | 4.68/602  | -2.62/516     | 647                     | 592    | 556                   | 495      |
| triethylamine                                    | 2.42                              | 50                 | 2.93/652  | 4.36/603  | -2.48/525     | 648                     | 591    | 556                   | 495      |
| dichloromethane <sup>l</sup>                     | 8.93                              |                    |   |           |               |                         |        |                       |          |
| tetrachloromethane                               | 2.23                              | 87.5               | 0.06/642  | 0.05/614  | -0.03/521     | 650 sh                  | 590 sh | 560 sh                | <i>k</i> |
| toluene  | 2.38                              | 87.5               | 0.31/661  | 0.37/606  | -0.27/532     | 650 sh                  | 596    | 560 sh                | <i>k</i> |
| benzene <sup>l</sup>                             | 2.27                              |                    |   |           |               |                         |        |                       |          |
| hexane   | 1.88                              | 60                 | 1.99/655  | 2.46/607  | -1.67/534     | 649                     | 596    | 558                   | 495      |

<sup>a</sup> Poly-1a: concentration, 0.25 mg/mL; cell length, 0.1 cm. <sup>b</sup> Relative permittivity (dielectric constant) for the pure liquid at 25 °C. <sup>c</sup> Percent volume of various solvents. <sup>d</sup> "sh" represents a shoulder peak. <sup>e</sup> Poly-1a concentration: 0.20–0.89 mg/mL. <sup>f</sup> It gave a hypsochromic shift. <sup>g</sup> It gave an almost opposite CD pattern compared with those in CHCl<sub>3</sub>–CH<sub>3</sub>OH mixtures. <sup>h</sup> It gave unusual CD changes compared with those in CHCl<sub>3</sub>–CH<sub>3</sub>OH mixtures. <sup>i</sup> It could not be measured due to absorption of the solvent. <sup>j</sup> It gave changes in CD pattern depending on the volume. <sup>k</sup> The UV–visible spectral changes were too little to estimate the isosbestic point. <sup>l</sup> No ICDs.



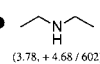
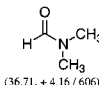
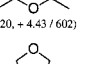
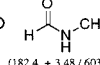
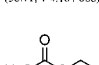
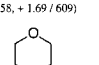
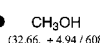
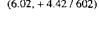
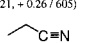
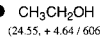
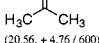
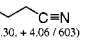
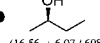
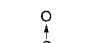
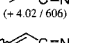
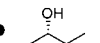
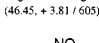
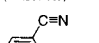
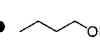
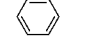
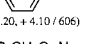
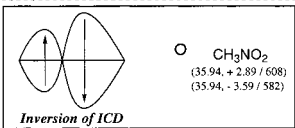
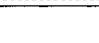
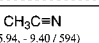
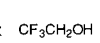
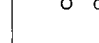

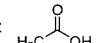
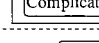
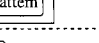
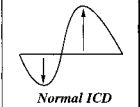

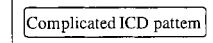
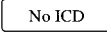
**Figure 4.** CD (A, C) and absorption (B, D) spectral changes of poly-1a in chloroform–acetonitrile (A, B) and chloroform–nitromethane (C, D) mixtures in a 0.1 cm quartz cell at ambient temperature (ca. 22–24 °C) with a poly-1a concentration of 0.25 mg (1.0  $\mu$ mol monomer units)/mL.

ICDs in their patterns and intensities compared with those in the chloroform–acetonitrile mixtures, indicating no isotope effect. We further examined a series of monohalogenated acetonitriles (fluoroacetonitrile, chloroacetonitrile, bromoacetonitrile, and iodoacetonitrile). Fluoroacetonitrile has a strong electronegative fluorine atom and it induced almost the same ICD on poly-1a with respect to its pattern, but the ICD intensity

decreased to approximately  $1/30$ th. On the other hand, the addition of bromoacetonitrile brought about the ICD on poly-1a whose ICD pattern was almost the same as that induced by methanol, while chloroacetonitrile caused a series of complicated ICDs differing from those by methanol and acetonitrile. CD measurements were very difficult in iodoacetonitrile because of its long absorption. Therefore, slight differences in the electro-



**Table 2. Relationships between Solvent Properties and Induced Cotton Effects on Poly-1a<sup>a</sup>**

| protic solvents  | dipolar aprotic solvents  | apolar aprotic solvents  |
|--|---|--|
| <br>(3.78, + 4.68 / 602)  | <br>(36.71, + 4.16 / 606)                          | <br>(4.20, + 4.43 / 602)  |
| <br>(182.4, + 3.48 / 603) | <br>(7.58, + 1.69 / 609)                           | <br>(2.42, + 4.36 / 603)  |
| <br>(32.66, + 4.94 / 608) | <br>(6.02, + 4.42 / 602)                           | <br>(2.21, + 0.26 / 605)  |
| <br>(24.55, + 4.64 / 606) | <br>(20.56, + 4.76 / 600)                          | <br>(28.86, + 3.94 / 607) |
| <br>(16.56, + 6.07 / 608) | <br>(46.45, + 3.81 / 605)                          | <br>(20.30, + 4.06 / 603) |
| <br>(16.56, + 5.91 / 608) | <br>(34.78, + 1.30 / 610)                          | <br>(+ 4.02 / 606)        |
| <br>(17.51, + 5.15 / 608) | <br>(25.20, + 4.10 / 606)                          | <br>(+ 4.20 / 605)        |
|                           | <br>(35.94, + 2.89 / 608)<br>(35.94, - 3.59 / 582) | <br>(+ 2.80 / 608)        |
| <br>(6.17)                | <br>(- 3.13 / 475)<br>(- 1.09 / 448)               | <br>(4.81)                |
| <br>(6.17)                | <br>(2.27)   | <br>(8.93)                |
|  |    | <br>(2.27)              |
|  |    |  |
|  |   |  |

<sup>a</sup> Relative permittivity (dielectric constant,  $\epsilon_r$ ) for the pure liquid if available and molar ellipticity ( $[\theta]_{\max} \times 10^{-4}$  (degree  $\text{cm}^2 \text{dmol}^{-1}$ ))/ $\lambda_{\max}$  (nm) of the first Cotton effect were shown in parentheses. The symbols denote the ICD intensities ( $[\theta]_{\max}$ ): (★)  $[\theta] > 7 \times 10^4$ ; (●)  $4 \times 10^4 < [\theta] \leq 7 \times 10^4$ ; (○)  $2 \times 10^4 < [\theta] \leq 4 \times 10^4$ ; (Δ)  $0 < [\theta] \leq 2 \times 10^4$ ; (×)  $[\theta] \approx 0$ .

static effects (electronegativity, dipole moment, and polarization) and size (van der Waals radius) of the poor solvents significantly influenced the chiroptical properties of the chiral supramolecular aggregates of poly-1a, although the reasons for this are still not completely elucidated.

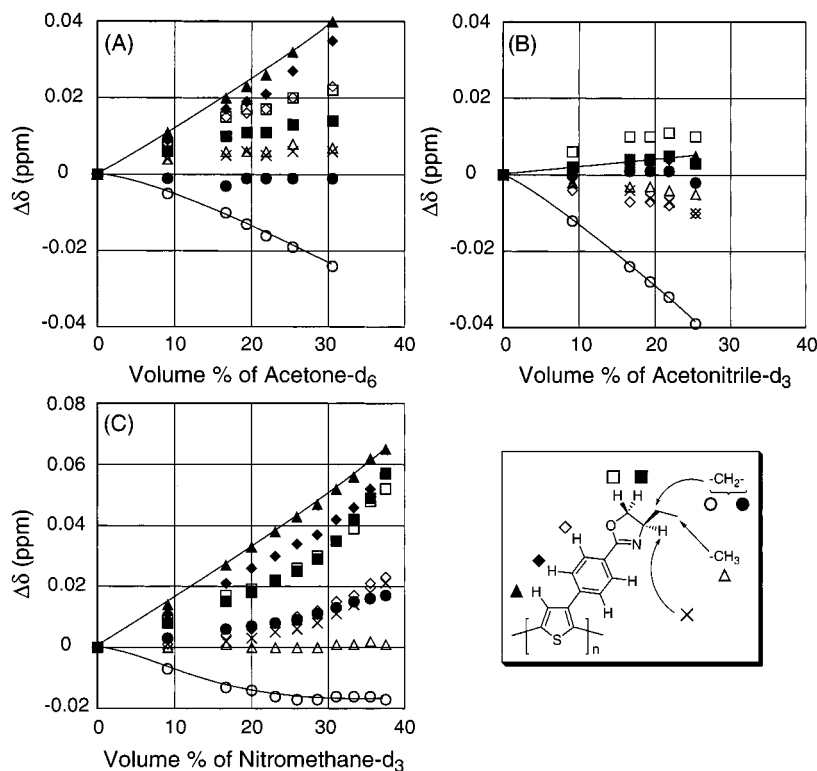
Nitromethane (30–70%, v/v) caused an inversion of the Cotton effects of poly-1a during the titration (Figure 4).<sup>18,20,21</sup> Poly-1a exhibited the same ICDs as those in the chloroform–methanol mixtures upon the addition of nitromethane (30–40%) and the solution color immediately changed from yellow-orange to purple. Further addition of nitromethane (50–70%) brought about an inversion of the ICDs with a negative first Cotton effect and a positive second Cotton effect accompanied by the slight blue-shift of  $\lambda_{\max}$  from 558 to 548 nm in the UV–visible spectra. This suggests that poly-1a may chirally aggregate with an opposite screw sense in a complicated mechanism depending not only on the properties of the solvents, but also on their volume ratios. Upon the addition of nitrobenzene, poly-1a exhibited the same ICD changes as those in the chloroform–methanol mixtures, and no inversion of the ICDs was observed.

Table 2 summarizes the relationships between the ICD patterns and the intensities of poly-1a and the polarity of the solvents used in these experiments according to Parker's classification.<sup>16,17</sup> Most protic

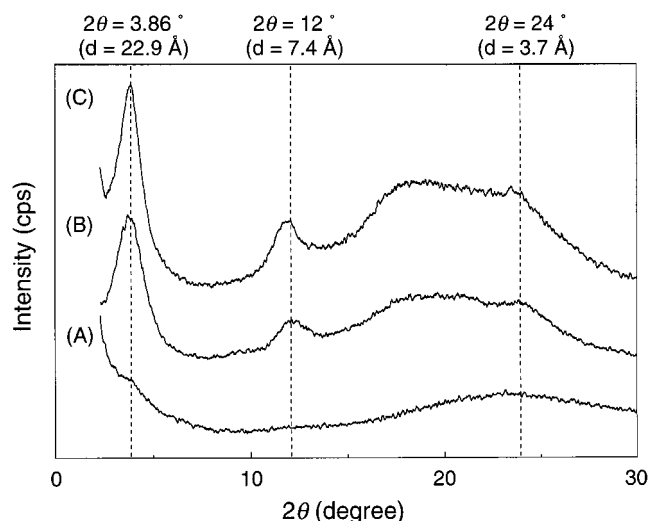
solvents except for acidic solvents such as acetic acid and 2,2,2-trifluoroethanol induced intense (marked by ● and ○ in Table 2) and normal ICDs on poly-1a, while apolar aprotic solvents tended to exhibit weak or no ICDs on poly-1a except for Et<sub>3</sub>N and hexane. On the other hand, the chiroptical properties of poly-1a were significantly influenced by the properties of the dipolar aprotic solvents, although most solvents except for 1,4-dioxane, THF, and nitrobenzene induced intense ICDs. In particular, some poor solvents such as acetonitrile and nitromethane caused dramatic solvent effects on poly-1a, and the polymer showed quite different ICDs.

**<sup>1</sup>H NMR Titrations of Poly-1a with Various Poor Solvents.** To gain information related to the conformational changes in poly-1a and the structures of the chiral aggregates during the titrations with different poor solvents, we followed the changes in the <sup>1</sup>H NMR chemical shifts ( $\Delta\delta$ ) during the titration of the CDCl<sub>3</sub> solution of poly-1a with acetone-*d*<sub>6</sub>, acetonitrile-*d*<sub>3</sub>, and nitromethane-*d*<sub>3</sub> which brought about the different ICD changes (Figure 5). The peaks were assigned using 2D COSY experiments. Upon the addition of acetone-*d*<sub>6</sub> (0–30%, v/v), the resonances derived from the thiophene ring proton at the 4-position and two aromatic ring protons neighboring to the main chain shifted downfield (0.02–0.04 ppm) accompanied by broadening of the peaks, while these proton resonances hardly changed even in the presence of 25 vol % acetonitrile-*d*<sub>3</sub>. The addition of nitromethane-*d*<sub>3</sub> caused larger downfield shifts (0.05–0.07 ppm) of the thiophene ring proton at the 4-position, two aromatic ring protons, and the two methylene protons on the oxazoline ring. The downfield shifts of the aromatic and thiophene ring protons indicate that the main chains may form a  $\pi$ -stacked bilayer lamellar structure, and these protons could be deshielded by a ring current effect. In all of the titration experiments, one of the methylene protons of the ethyl group shifted upfield (0.02–0.04 ppm). The significant upfield shifts of the methylene protons imply that an aromatic ring may be closely located above the methylene protons so that it can substantially affect the ring current effect. Unfortunately, upon further addition of these poor solvents, poly-1a precipitated under the present conditions. The different changes in the <sup>1</sup>H NMR chemical shifts must be correlated to the difference in the structures of the chiral aggregates depending on the nature of the solvents which cause the differences in the ICD changes.

**X-ray Diffraction of Poly-1a.** To investigate the effect of poor solvents on the structures and packing modes for poly-1a, X-ray diffraction measurements of the poly-1a powders prepared from chloroform solutions of poly-1a with methanol, acetone, and acetonitrile (50/50, v/v) were performed (Figure 6).<sup>2,5,22</sup> A chloroform-cast film revealed a rather amorphous structure with a broad peak at  $2\theta = \text{ca. } 24^\circ$  corresponding to a diffuse halo from the scattering of the glass substrate and partially from the 3.7 Å  $\pi$ -stacking space (Figure 6A). A very weak peak at  $3.86^\circ$  was also observed which could be identified as the first-order (1,0,0) parallel spacing of the main chain reflection ( $d = 22.9$  Å) for the cast film. However, the reflection intensity at  $2\theta = \text{ca. } 3.86^\circ$  dramatically increased for the powdered samples prepared from the chloroform–acetone and chloroform–acetonitrile mixtures (Figure 6, parts B and C). New peaks at  $2\theta = \text{ca. } 12^\circ$  ( $d = 7.4$  Å) corresponding to parallel spacing of the main chains (3,0,0) and at ca.



**Figure 5.** Changes in  $^1\text{H}$  NMR chemical shifts of poly-**1a** in  $\text{CDCl}_3$  upon addition of acetone- $d_6$  (A), acetonitrile- $d_3$  (B), and nitromethane- $d_3$  (C) at ambient temperature (ca. 22–24 °C). An initial poly-**1a** concentration was 2 mg (8  $\mu\text{mol}$  monomer units)/mL. Negative values indicate an upfield shift.



**Figure 6.** X-ray diffractograms for the cast film prepared from chloroform (A) and for the powder samples precipitated from chloroform–acetone (B) and chloroform–acetonitrile (C) (50/50, v/v) mixtures of poly-**1a**.

$24^\circ$  ( $d = 3.7 \text{ \AA}$ ) corresponding to the face-to-face  $\pi$ -stacked spacing were also observed. Similar XRD patterns were reported for other regioregular polythiophenes.<sup>22</sup> It may be difficult to investigate the influence of poor solvents on the chiral structures and packing modes for poly-**1a** by means of X-ray diffraction, because the diffraction patterns of the prepared powders from different solvent mixtures were relatively similar to each other, while the reflection peaks for the sample obtained from the chloroform–acetonitrile mixture are slightly sharper and more intense than those precipitated from acetone.

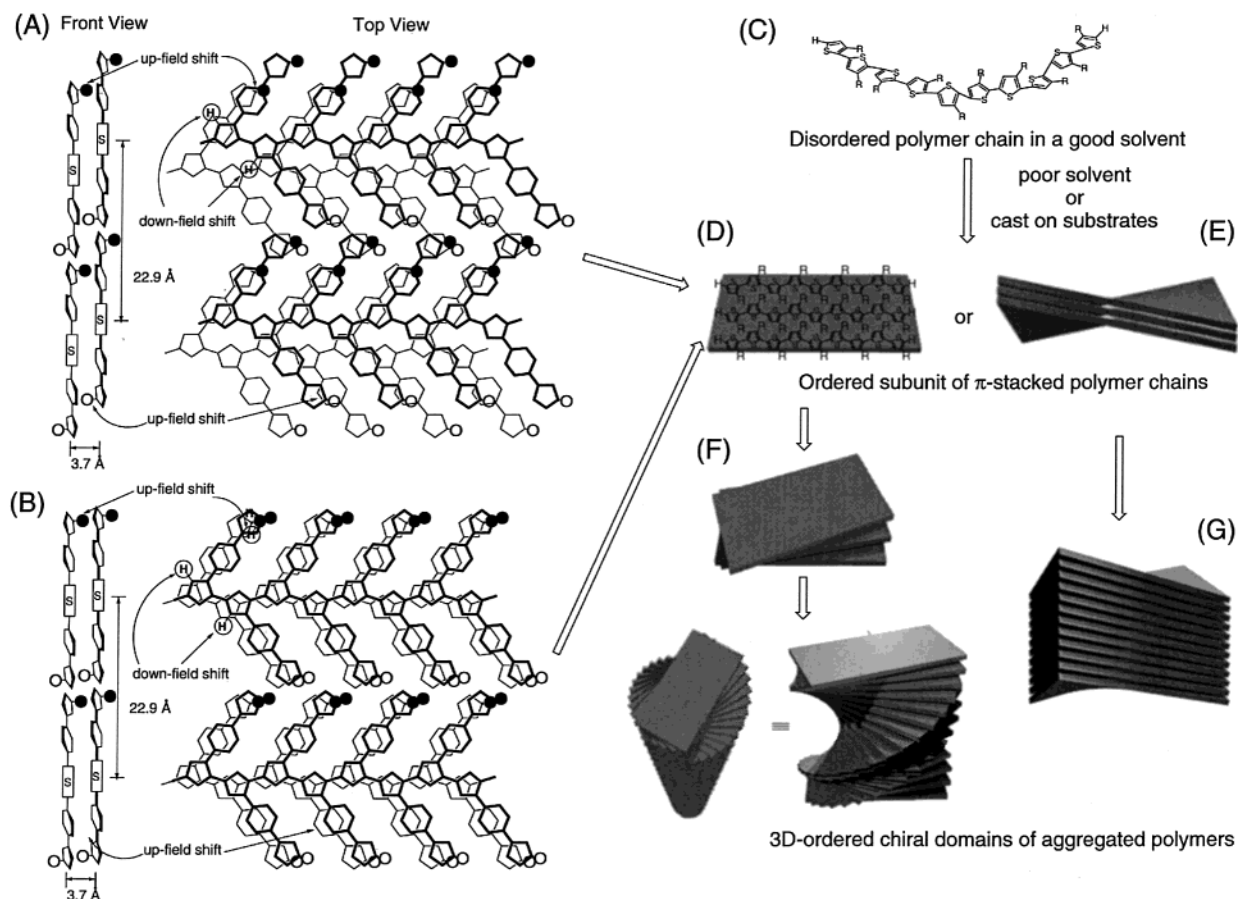
The UV–visible and CD spectra of the poly-**1a** cast films prepared from the same solvent mixtures on a

quartz cell were then measured. These films exhibited almost the same UV–visible spectra as each other and similar to those in solutions containing excess poor solvents (Figures 2 and 4). Moreover, the cast films from the chloroform–methanol, –acetone, and –acetonitrile mixtures showed intense, split-type ICDs whose ICD patterns were almost the same as those in solution. These results indicate that the poly-**1a** may have similar structures and packing modes in the precipitated powders, cast films, and aggregates in solution.

**Model of Poly-1a Aggregates.** The XRD, NMR, and UV–visible, and CD experiments demonstrate that poly-**1a** is aggregated to form a  $\pi$ -stacked, chiral supramolecular assembly through intermolecular interactions in the presence of poor solvents. Because of the few diffraction peaks for the chiral aggregates independent of a poor solvent, a precise model for the chiral supramolecular structures of poly-**1a** cannot be drawn. However, a model can be proposed using the XRD and NMR data of the poly-**1a** aggregates combined with the reported structural data of the regioregular achiral poly-(3-alkylthiophene)s determined by XRD analyses,<sup>22</sup> together with computer modeling.

The poly-**1a** aggregates showed typical reflections which correspond to a well-ordered lamellar structure with an interlayer spacing of 22.9  $\text{\AA}$  and a stacking distance of the two polymer chains of 3.7  $\text{\AA}$ . Figure 7A illustrates a schematic structure based on computer modeling using molecular mechanics calculations. The molecules have been arranged in Figure 7A to fit the XRD and NMR data. The polythiophene backbones are assumed to be planar and packed in the end-to-end mode. The phenyl rings are slightly twisted to avoid a sterically unfavorable interaction. The intermolecular  $\pi$ -stacked aggregations may occur through the face-to-face thiophene–aromatic interactions, which bring about





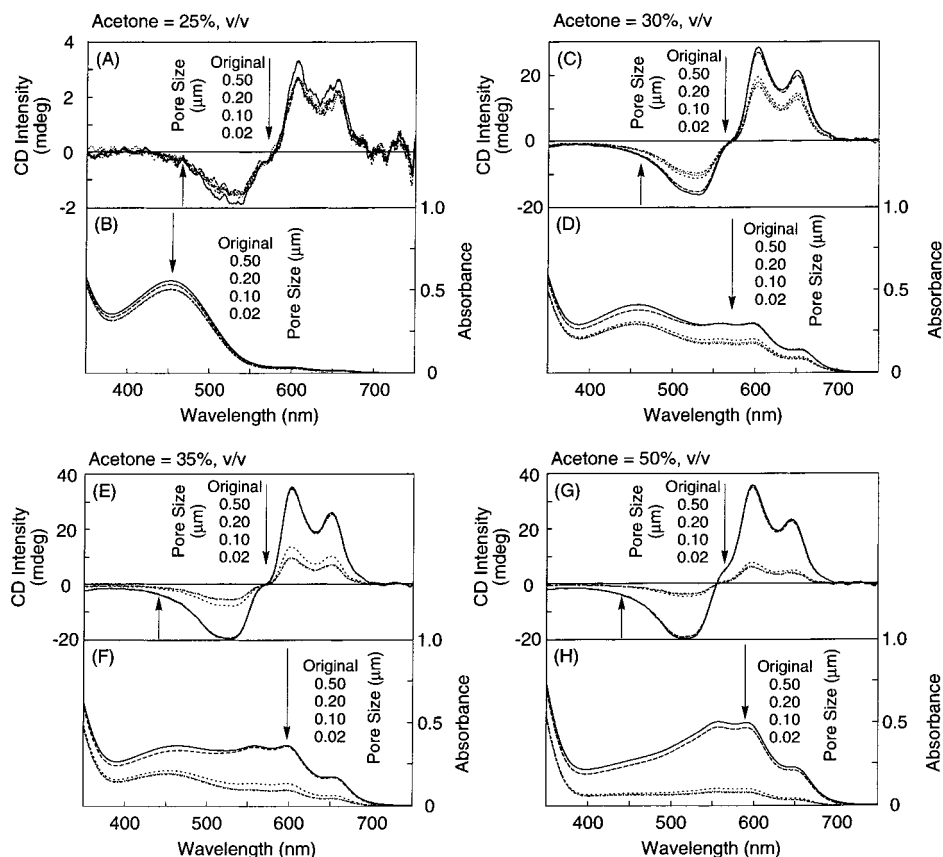
**Figure 7.** Possible models (A and B) and the steps in the formation of chiral poly-1a aggregates (C–G).

the bathochromic shift of the absorption band (Figures 2 and 4). The interchain  $\pi$ – $\pi$  stacking of the polythiophene main chain (thiophene–thiophene) (Figure 7B) could not be ruled out. However, the model in Figure 7A explains the upfield shifts of the methylene protons (○ and ●) of the ethyl group of the oxazoline residues and the downfield shift of the thiophene ring proton; the phenyl ring is favorably positioned above or below the methylene protons and the thiophene proton may be located close to the phenyl rings so that the proton is deshielded by the ring current effect.

The supramolecular assembly process of poly-1a in poor solvents is schematically illustrated in Figure 7, parts C–G. Upon the addition of a poor solvent, poly-1a self-assembles to aggregate into an ordered chiral subunit (Figure 7D) associated with a conformational change from a disordered (Figure 7C) to an ordered form. Attractive interlayer  $\pi$ -stacking interactions must play a central role in the self-assembling process. The supramolecular chirality may be induced on the laminated poly-1as during further aggregation; each layer may be loosely twisted clockwise or counterclockwise depending on poor solvents so that the poly-1a aggregates exhibit optical activity (Figure 7F), thus showing exciton-type splitting Cotton effects.<sup>23</sup> Another possible model for the optical activity is shown in Figure 7, parts E and G; the  $\pi$ -stacked interlayer main chains of poly-1a may be quite loosely twisted in one direction (Figure 7E). Here, the optical activity originates from the twisted poly-1a molecule alone. However, further intermolecular  $\pi$ -stacked self-assemblies may be necessary for clustering in the  $\pi$ -stacks (Figure 7G).

**Filtration Experiments of Poly-1a in Various Solvents Mixtures.** To obtain information with respect

to the particle sizes of the chiral poly-1a aggregates in chloroform in the presence of poor solvents, the poly-1a solutions containing acetone, acetonitrile, or nitromethane were filtered through the membrane filters with pore sizes of 0.50, 0.20, 0.10, and 0.02  $\mu\text{m}$  and the particle sizes were estimated by measuring the intensity changes of the filtrates in the CD and absorption spectra,<sup>2</sup> since light scattering measurements were difficult due to the intense absorption around the laser beam (632.8 nm). Figure 8 shows the changes in the CD and absorption spectra for the poly-1a solutions using the series of membrane filters. In all the experiments, the changes of the filtrates in the CD spectra agree with those in the absorption spectra. The chloroform solution of poly-1a passed through the membrane with the pore size of 0.02  $\mu\text{m}$ , while the aggregated poly-1a in the chloroform-poor solvents mixtures could not pass through the membrane with smaller pore sizes because the size of the particles formed increased with the increasing amount of acetone (Figure 8 (parts A–H)). In the presence of 25 vol % acetone, most of the poly-1a permeated through the membrane (0.02  $\mu\text{m}$ ), but the filtrate exhibited a slight decrease in the ICD intensity. A further decrease in the CD and absorption intensities was observed upon the addition of an increasing amount of acetone. When the content of acetone is increased to 50% (v/v) (Figure 8 (parts G and H)), more than 90% of poly-1a could pass through the membranes (0.50  $\mu\text{m}$  pore), but only about 20% of poly-1a passed through the membrane with a pore size of 0.20  $\mu\text{m}$ . The absorption and CD patterns of the filtrates hardly changed compared with those before filtration, indicating that the size of the chiral aggregates is substantially independent of the electronic and chirop-



**Figure 8.** CD (A, C, E, G) and absorption (B, D, F, H) spectral changes of poly-**1a** in chloroform–acetone mixtures after filtration through membrane filters with pore size of 0.50, 0.20, 0.10, and 0.02  $\mu\text{m}$ . Acetone content is 25 (A, B), 30 (C, D), 35 (E, F), and 50% (v/v) (G, H). All spectra were measured in a 0.5 cm quartz cell at ambient temperature (ca. 22–24  $^{\circ}\text{C}$ ) with a poly-**1a** concentration of 0.05 mg (0.2  $\mu\text{mol}$  monomer units)/mL before filtration.

**Table 3. Absorbance Changes of Poly-1a Solution after Filtration through Membrane Filters<sup>a</sup>**

| solvent      | v, % <sup>b</sup> | initial absorbance before filtration ( $\lambda$ (nm)) | % decrease in absorbance after filtration <sup>c</sup> for pore size of membrane filters ( $\mu\text{m}$ ) |      |      |      |
|--------------|-------------------|--|--|------|------|------|
|              |                   |  | 0.50   | 0.20 | 0.10 | 0.02 |
| acetone      | 25                | 0.038 (596)  | 3.8  | 20.1 | 22.4 | 23.7 |
|              | 30                | 0.304 (596)  | 1.4  | 31.7 | 38.2 | 41.3 |
|              | 35                | 0.367 (596)  | 1.8  | 62.3 | 72.9 | 73.5 |
|              | 50                | 0.501 (591)  | 6.1  | 79.4 | 83.2 | 84.0 |
| acetonitrile | 20                | 0.098 (552)  | 5.7  | 20.7 | 27.6 | 29.7 |
|              | 25                | 0.287 (552)  | 0.6  | 41.6 | 60.7 | 64.3 |
|              | 30                | 0.460 (552)  | 3.8  | 76.3 | 92.1 | 97.6 |
|              | 50                | 0.538 (552)  | 9.7  | 91.5 | 99.2 | 99.2 |
| nitromethane | 30                | 0.286 (558)  | 33.6   | 43.5 | 83.1 | 93.7 |
|              | 45                | 0.456 (558)  | 58.8   | 63.6 | 71.1 | 97.8 |
|              | 50                | 0.472 (555)  | 79.7   | 83.4 | 88.8 | 99.6 |
|              | 60                | 0.488 (551)  | 88.1   | 91.7 | 97.1 | 99.7 |

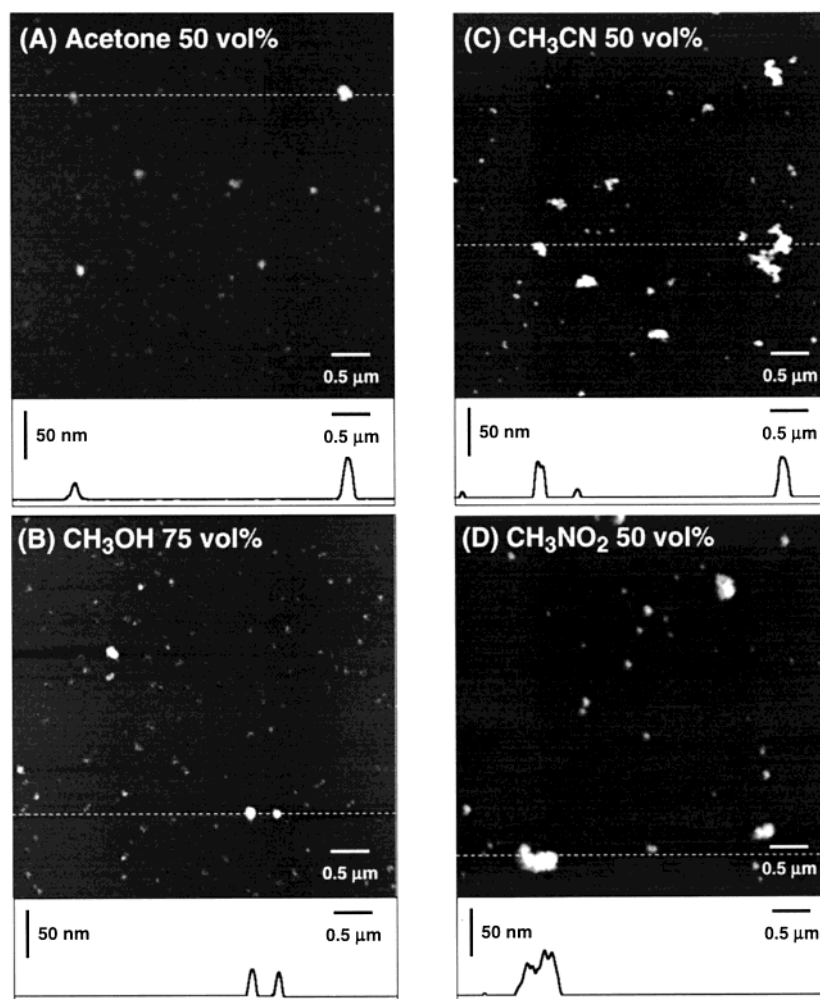
<sup>a</sup> Concentration of poly-**1a** before filtration is 0.05 mg/mL (0.2 mM monomer units). <sup>b</sup> Percent volume of poor solvents. <sup>c</sup>  $(A_b - A_a)/A_b \times 100$ :  $A_a$  = absorbance after filtration;  $A_b$  = absorbance before filtration.

tical properties of the aggregates. These filtration experiments reveal that the size of the particle in the poly-**1a** aggregates is larger than 0.02  $\mu\text{m}$  and approximately in the range of 0.20 to 0.50  $\mu\text{m}$ .

Table 3 summarizes the filtration experiment results showing the changes in the absorption intensity of the chloroform solution of poly-**1a** after filtration upon the addition of acetone, acetonitrile, and nitromethane. When acetonitrile and nitromethane were used as the poor solvents, larger particles of poly-**1a** formed in a relatively small amount of the poor solvents and the aggregated poly-**1a** molecules could not pass through the membrane with a pore size of 0.02  $\mu\text{m}$  in the chloroform with 30% acetonitrile and nitromethane. The ICD patterns exhibited no change before and after the

filtrations. The results of the filtration experiments suggest that the size of the chiral supramolecular aggregates of poly-**1a** is largely dependent not only on the nature of the solvents, but also on their volume ratios. However, the relationships between the size of the poly-**1a** aggregates and ICD patterns are not still clear at present.

**AFM Measurements of Poly-1a Aggregates.** AFM measurements were carried out to directly estimate the sizes of the chiral poly-**1a** aggregates in various chloroform solvent mixtures (Figure 9) in the tapping mode.<sup>24</sup> The AFM images show a number of small round particles with diameters of less than 0.1  $\mu\text{m}$  together with a few large particles (0.2–0.3  $\mu\text{m}$ ) in mixtures of chloroform and acetone or methanol. On the other hand,



**Figure 9.** AFM images of poly-**1a** on mica substrates prepared from chloroform–acetone (A), chloroform–methanol (B), chloroform–acetonitrile (C), and chloroform–nitromethane mixtures (D). Percent volumes of the poor solvents to chloroform are 50 (A, C, D) and 75 (B).

the size of the chiral aggregates of poly-**1a** in the presence of acetonitrile and nitromethane as poor solvents is approximately in the range 0.3–0.5  $\mu\text{m}$ , and small particles of less than 0.1  $\mu\text{m}$  as observed in the chloroform–methanol mixtures were minor aggregates. Similar particle-size distributions of the poly-**1a** aggregates were mostly observed in other places on the mica substrates. These results agree with the experimental filtration results. However, it is still difficult to differentiate the conformation or packing mode of the chiral supramolecular aggregates of poly-**1a** formed in different poor solvent mixtures by AFM.

## Conclusion

We found dramatic changes in the CD and absorption spectra of a chiral regioregular polythiophene derivative bearing an optically active oxazoline residue (poly-**1a**) depending on the nature of the solvents and their volume ratios. Upon the addition of poor solvents to the chloroform solution of poly-**1a**, the polymer forms chiral, supramolecular self-assemblies with different handedness accompanied by the transformation of the polymer conformation. Moreover, the size and state of the aggregates are different depending on the solvents based on the  $^1\text{H}$  NMR titrations, X-ray diffraction analysis, filtration experiments with membrane filters, and AFM measurements. This study may be among the most extensive stereochemical ones to date concerning

the effects of poor solvents on the structures of the chiral polythiophene aggregates. Nevertheless, we are unable to provide a complete structural interpretation of the molecular origin of chirality induction on the poly-**1a** aggregates at the present stage, although a possible model for the supramolecular aggregates could be proposed based on the spectroscopic results. To elucidate the structures of the chiral aggregates induced by poor solvents at a molecular level, further studies using a series of chiral oligomers of poly-**1a** with a well-defined structure may be useful.<sup>15</sup> This work is now in progress.

**Acknowledgment.** We thank Professor T. Hattori and Y. Inaki (Nagoya University) for their help in the X-ray diffraction measurements. This work was partially supported by a Grant-in-Aid for Scientific Research from the Japan Society for the Promotion of Science (JSPS) and the Ministry of Education, Culture, Sports, Science, and Technology, Japan. H.G. expresses thanks for a JSPS Research Fellowship (No. 00857) for Young Scientists.

## References and Notes

- (1) (a) Reichardt, C. *Solvents and Solvent Effects in Organic Chemistry*; VCH: Weinheim, Germany, 1990; Chapter 6, pp 285–337. (b) Suppan, P.; Ghoneim, N. *Solvatochromism*; The Royal Society of Chemistry: Cambridge, England, 1997. (c) Rughoputh, S. D. D. V.; Hotta, S.; Heeger, A. J.; Wudl, F. *J.*



- Polym. Sci., Polym. Phys. Ed.* **1987**, 25, 1071–1078. (d) Faïd, K.; Fréchette, M.; Ranger, M.; Mazerolle, L.; Lévesque, I.; Leclerc, M.; Chen, T.-A.; Rieke, R. D. *Chem. Mater.* **1995**, 7, 1390–1396.
- (2) Yamamoto, T.; Komarudin, D.; Arai, M.; Lee, B.-L.; Suganuma, H.; Asakawa, N.; Inoue, Y.; Kubota, K.; Sasaki, S.; Fukuda, T.; Matsuda, H. *J. Am. Chem. Soc.* **1998**, 120, 2047–2058.
- (3) (a) Patil, A. O.; Heeger, A. J.; Wudl, F. *Chem. Rev.* **1988**, 88, 183–200. (b) Roncali, J. *Chem. Rev.* **1992**, 92, 711–738. (c) Yamamoto, T. *Prog. Polym. Sci.* **1992**, 17, 1153–1205. (d) Berggren, M.; Inganäs, O.; Gustafsson, G.; Rasmussen, J.; Andersson, M. R.; Hjertberg, T.; Wennerström, O. *Nature* **1994**, 372, 444–446. (e) Roncali, J. *Chem. Rev.* **1997**, 97, 173–205. (f) Goldenberg, L. M.; Bryce, M. R.; Petty, M. C. *J. Mater. Chem.* **1999**, 9, 1957–1974. (g) McQuade, D. T.; Pullen, A. E.; Swager, T. M. *Chem. Rev.* **2000**, 100, 2537–3574. (h) Kim, D. Y.; Cho, H. N.; Kim, C. Y. *Prog. Polym. Sci.* **2000**, 25, 1089–1139.
- (4) (a) Lemaire, M.; Delabouglise, D.; Garreau, G.; Guy, A.; Roncali, J. *J. Chem. Soc., Chem. Commun.* **1988**, 658–661. (b) Bouman, M. M.; Havinga, E. E.; Janssen, R. A. J.; Meijer, E. W. *Mol. Cryst. Liq. Cryst.* **1994**, 256, 439–448. (c) Bouman, M. M.; Meijer, E. W. *Adv. Mater.* **1995**, 7, 385–387. (d) Langeveld-Voss, B. M. W.; Janssen, R. A. J.; Christiaans, M. P. T.; Meskers, S. C. J.; Dekkers, H. P. J. M.; Meijer, E. W. *J. Am. Chem. Soc.* **1996**, 118, 4908–4909. (e) Pu, L. *Acta Polym.* **1997**, 48, 116–141. (f) Ochiai, K.; Tabuchi, Y.; Rikukawa, M.; Sanui, K.; Ogata, N. *Thin Solid Films* **1998**, 327–329, 454–457. (g) Langeveld-Voss, B. M. W.; Christiaans, M. P. T.; Janssen, R. A. J.; Meijer, E. W. *Macromolecules* **1998**, 31, 6702–6704. (h) Kilbinger, A. F. M.; Schenning, A. P. H. J.; Goldoni, F.; Feast, W. J.; Meijer, E. W. *J. Am. Chem. Soc.* **2000**, 122, 1820–1821. (i) Iarossi, D.; Mucci, A.; Parenti, F.; Schenetti, L.; Seeber, R.; Zanardi, C.; Forni, A.; Tonelli, M. *Chem.-Eur. J.* **2001**, 7, 676–685. (j) Zhang, Z.-B.; Fujiki, M.; Motonaga, M.; Nakashima, H.; Torimitsu, K.; Tang, H.-Z. *Macromolecules* **2002**, 35, 941–944.
- (5) Langeveld-Voss, B. M. W.; Janssen, R. A. J.; Meijer, E. W. *J. Mol. Struct.* **2000**, 521, 285–301.
- (6) Yashima, E.; Goto, H.; Okamoto, Y. *Macromolecules* **1999**, 32, 7942–7945.
- (7) Goto, H.; Yashima, E.; Okamoto, Y. *Chirality* **2000**, 12, 396–399.
- (8) (a) Bouman, M. M.; Meijer, E. W. *Adv. Mater.* **1995**, 7, 385–387. (b) Trznadel, M.; Pron, A.; Zagorska, M.; Chrzascz, R.; Pielichowski, J. *Macromolecules* **1998**, 31, 5051–5058.
- (9) (a) McCullough, R. D.; Lowe, R. D.; Jayaraman, M.; Anderson, D. L. *J. Org. Chem.* **1993**, 58, 904–912. (b) McCullough, R. D.; Williams, S. P. *J. Am. Chem. Soc.* **1993**, 115, 11608–11609. (c) McCullough, R. D. *Adv. Mater.* **1998**, 10, 93–116.
- (10) (a) Mayo, S. L.; Olafson, B. D.; Goddard, W. A., III. *J. Phys. Chem.* **1990**, 94, 8897–8909. (b) Rappé, A. K.; Goddard, W. A., III. *J. Phys. Chem.* **1991**, 95, 3358–3363.
- (11) Ahn, K. H.; Cho, C.-W.; Beak, H.-H.; Park, J.; Lee, S. *J. Org. Chem.* **1996**, 61, 4937–4943.
- (12) (a) Miyaaura, N.; Suzuki, A. *Chem. Rev.* **1995**, 95, 2457–2483. (b) Wang, X.-Z.; Deng, M.-Z. *J. Chem. Soc., Perkin Trans. 1* **1996**, 2663–2664.
- (13) (a) Miyazaki, Y.; Yamamoto, T. *Synth. Met.* **1994**, 64, 69–79. (b) Yamamoto, T.; Oguro, D.; Kubota, K. *Macromolecules* **1996**, 29, 1833–1835. (c) Yamamoto, T.; Hayashi, H. *J. Polym. Sci., Part A: Polym. Chem.* **1997**, 35, 463–474.
- (14) The protons at the 4-position on the thiophene ring of poly-(3-substituted thiophene)s are expected to resonate as four singlets at around 6.8–7.2 ppm reflecting their trimeric sequences (Chart 1). However, the end groups resonances overlapped with these singlets, and therefore, precise regio-regularity could not be determined.
- (15) Sakurai, S.; Goto, H.; Yashima, E. *Org. Lett.* **2001**, 3, 2379–2382.
- (16) Reichardt, C. *Solvents and Solvent Effects in Organic Chemistry*; VCH: Weinheim, Germany, 1990; Chapter 3, pp 51–77.
- (17) Reichardt, C. *Solvents and Solvent Effects in Organic Chemistry*; VCH: Weinheim, Germany, 1990, appendix, pp 407–437.
- (18) Langeveld-Voss, B. M. W.; Christiaans, M. P. T.; Janssen, R. A. J.; Meijer, E. W. *Macromolecules* **1998**, 31, 6702–6704.
- (19) Peeters, E.; Janssen, R. A. J.; Meskers, S. C. J.; Meijer, E. W. *Polym. Prepr.* **1999**, 40 (1), 519–520.
- (20) (a) Nakashima, H.; Fujiki, M.; Koe, J. R.; Motonaga, M. *J. Am. Chem. Soc.* **2001**, 123, 1963–1969. (b) Nakashima, H.; Koe, J. R.; Torimitsu, K.; Fujiki, M. *J. Am. Chem. Soc.* **2001**, 123, 4847–4848.
- (21) Bidan, G.; Guillerez, S.; Sorokin, V. *Adv. Mater.* **1996**, 8, 157–160.
- (22) (a) Fichou, D.; Ziegler, C. In *Handbook of Oligo- and Polythiophenes*; Fichou, D., Ed.; Wiley-VCH: Weinheim, Germany, 1999; Chapter 4, pp 183–282. (b) Prosa, T. J.; Winokur, M. J.; McCullough, R. D. *Macromolecules* **1996**, 29, 3654–3656. (c) Caronna, T.; Catellani, M.; Luzzati, S.; Meille, S. V.; Romita, V. *Macromol. Rapid Commun.* **1997**, 18, 939–943. (d) Tashiro, K.; Kobayashi, M.; Kawai, T.; Yoshino, K. *Polymer* **1997**, 38, 2867–2879. (e) Kobashi, M.; Takeuchi, H. *Macromolecules* **1998**, 31, 7273–7278. (f) Asamundtveit, K. E.; Samuelsen, E. J.; Guldstein, M.; Steinsland, C.; Flornes, O.; Fagermo, C.; Seeberg, T. M.; Pettersson, L. A. A.; Inganäs, O.; Feidenhans'l, R.; Ferrer, S. *Macromolecules* **2000**, 33, 3120–3127. (g) Hong, X. H.; Tyson, J. C.; Collard, D. M. *Macromolecules* **2000**, 33, 3502–3504. (h) Asamundtveit, K. E.; Samuelsen, E. J.; Mammo, W.; Svensson, M.; Andersson, M. R.; Pettersson, L. A. A.; Inganäs, O. *Macromolecules* **2000**, 33, 5481–5489. (i) Yamamoto, T.; Kokubo, H. *J. Polym. Sci., Part B: Polym. Phys.* **2000**, 38, 84–87.
- (23) Beljonne, D.; Langeveld-Voss, B. M. W.; Shuai, Z.; Janssen, R. A. J.; Meskers, S. C. J.; Meijer, E. W.; Brédas, J. L. *Synth. Met.* **1999**, 102, 912–913.
- (24) (a) Hempenius, M. A.; Langeveld-Voss, B. M. W.; van Haare, J. A. E. H.; Janssen, R. A. J.; Sheiko, S. S.; Spatz, J. P.; Möller, M.; Meijer, E. W. *J. Am. Chem. Soc.* **1998**, 120, 2798–2804. (b) Takeuchi, H.; Kobashi, M. *Chem. Lett.* **1999**, 415–416. (c) Reitzel, N.; Greve, D. R.; Kjaer, K.; Howes, P. B.; Jayaraman, M.; Savoy, S.; McCullough, R. D.; McDevitt, J. T.; Bjørnholm, T. *J. Am. Chem. Soc.* **2000**, 122, 5788–5800.

MA012083P